"Miniwatt"

DIGEST

VOL. 2. No. 4
JANUARY 1963

TECHNICAL AND COMMERCIAL TOPICS OF CURRENT INTEREST TO THE ELECTRONICS INDUSTRY

CONTENTS

QUALITY CONTROL OF MINIATURE GERMANIUM DIODES

Physical investigation of prepared section of cathode assembly using specialised microscope

Published by the "Miniwatt" Electronics Division of Philips Electrical Industries Pty. Limited, 20 Herbert Street, Artarmon, N.S.W., Australia

Production of Miniature Germanium Diodes

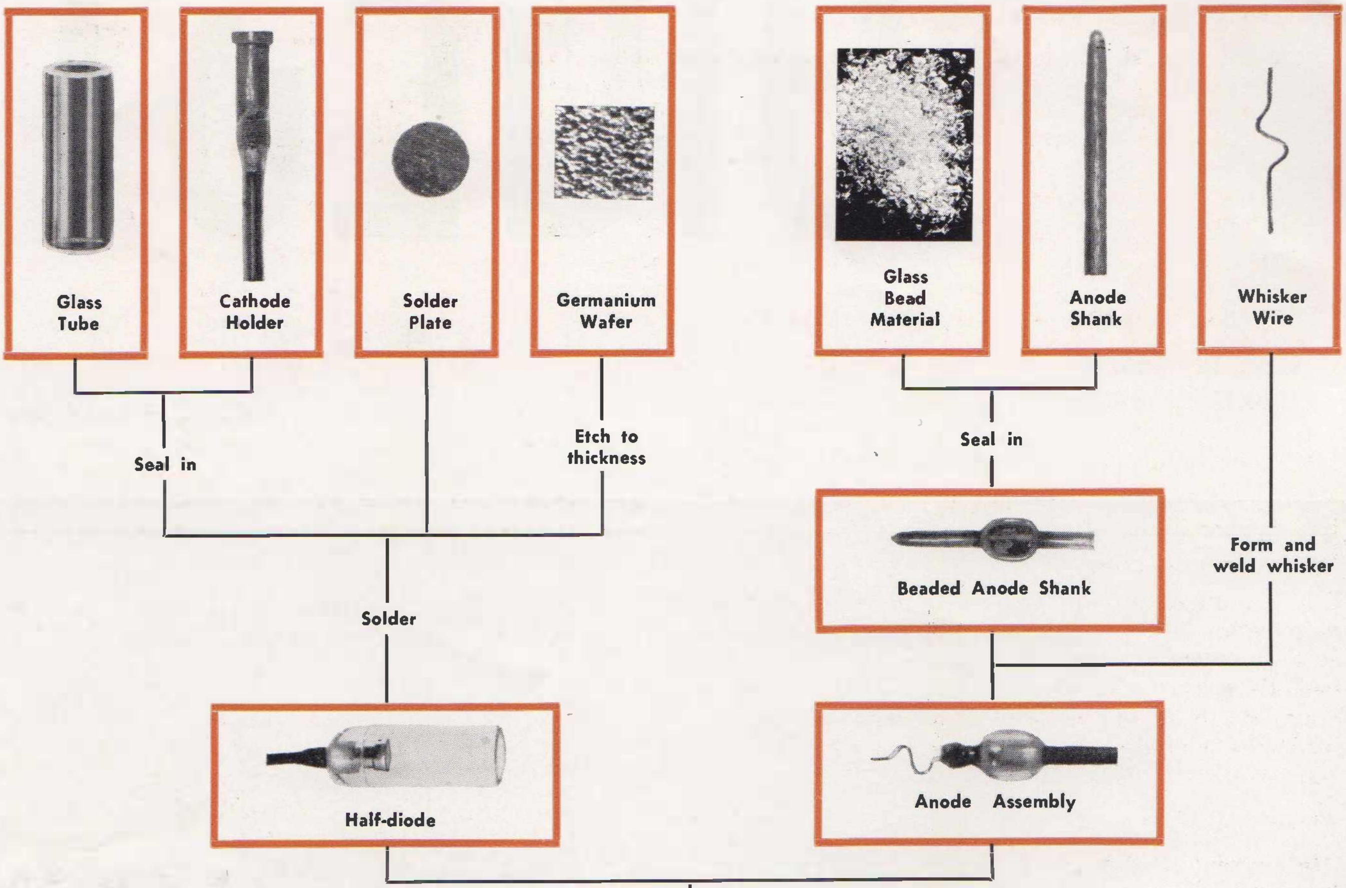

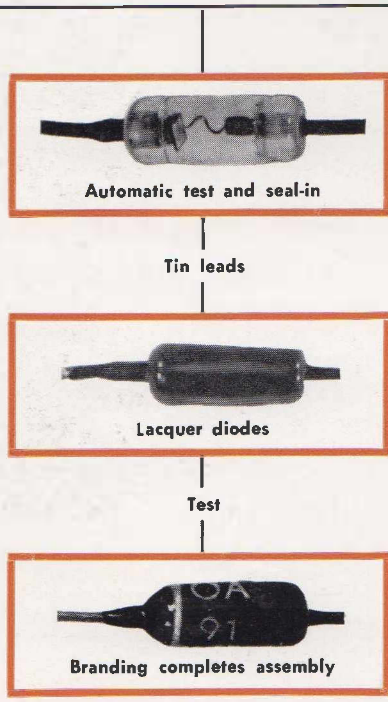

MANUFACTURING SCHEME OF MINIWATT MINIATURE DIODES

ACTUAL SIZE

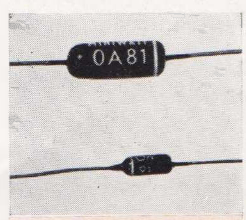

Fig. 1. Comparison in size between OA91 miniature diode and OA81 which it replaces.

in Australia

Germanium diode production commenced at the Hendon, South Australia, plant in September 1959. Since then millions of the "OA80" series diodes have been produced for both entertainment and professional applications.

Over the past year or two there has been a growing demand for miniature diodes in portable radios, ratio and video detector cans and professional equipment. With the development of new types to complete the range of Miniwatt miniature diodes it was decided to change over from the normal ("OA80") diode series to the miniature ("OA90") diode series, and these are now in full production at Hendon.

The manufacturing scheme is broadly as shown below. The emphasis placed on product quality is indicated by the extensive testing and quality control procedures described in the article.

REPLACEMENT LIST

Miniature Type		Electrically Equivalent Type
OA90	replaces	OA80 and OA70*
OA91	replaces	OA81 and OA74
OA95	replaces	OA85
AA119	replaces	OA79
2-AA119	replaces	2-OA79

* video detector service

MANUFACTURING PROCESSES

The stages in miniature diode manufacture are shown schematically on the opposite page, and the major processes are outlined below.

Half-Diode Assembly

The first stage of this assembly is to seal a copper cathode holder into a glass tube on a 12-head rotary sealing machine (Fig. 2). An etched germanium cathode of the type of diode required is then soldered on to the head of the cathode holder. The copper lead wire is used to give the lowest possible thermal resistance for the small diode.

Anode Assembly

After beading, the anode shank is cropped and flattened. Then either a tungsten or molybdenum wire is formed into an S-shape and welded on to the flat on an automatic machine (Fig. 3). The final stage is to etch the point of the whisker electrolytically to obtain the correct shape.

Final Assembly

The half-diode and anode assembly are brought together on a 48-head automatic testing and sealing machine (Fig. 4) which in sequence positions the whisker on the cathode, applies a fixed tension to the whisker, forms the junction with a powering pulse, tests the junction for forward and reverse voltage characteristics and rejects it if it is unsatisfactory. This sequence can be repeated up to three times in order to find a spot on the wafer which gives the correct characteristic. Diodes which pass all these tests are then sealed in and unloaded by the machine. The finally sealed diode is shown in the insert to Fig. 4.

Finishing and Testing

The sealed diodes have next to be finished by tinning the lead wires for easy solderability, and lacquered black to make them insensitive to light.

The diodes are then tested for their forward and reverse characteristics, and dynamically to detect any loop, flutter or drift. Certain diodes (namely the OA90 and AA119) are also checked for detection efficiency and damping resistance and paired if necessary (Fig. 5).

The final stage of production is to brand them with their type mark and cathode band.

Semiconductor Factory—Hendon

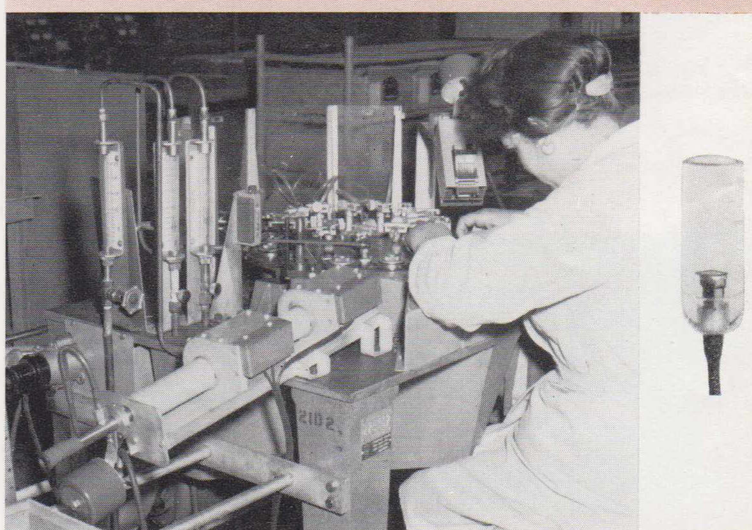

▲ Fig. 2. Twelve-head rotary machine for sealing glass tubes to cathode holders during manufacture of half-diodes. On right is a completely assembled half-diode.

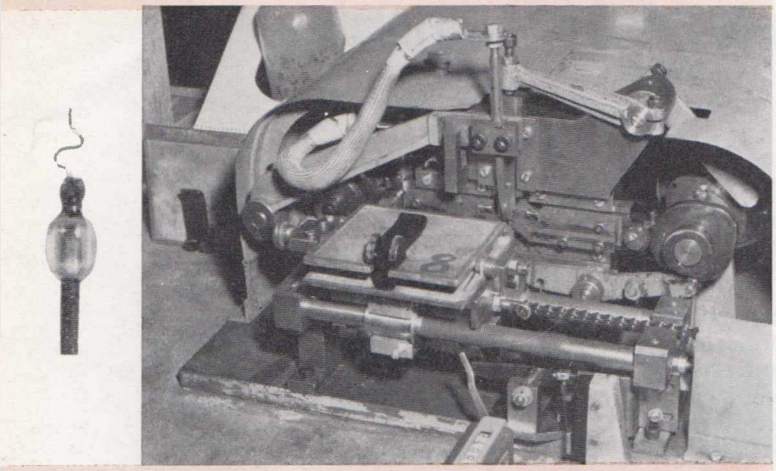

Fig. 3. Whisker forming and welding machine used during manufacture of anode assemblies. On left is a completed anode assembly.

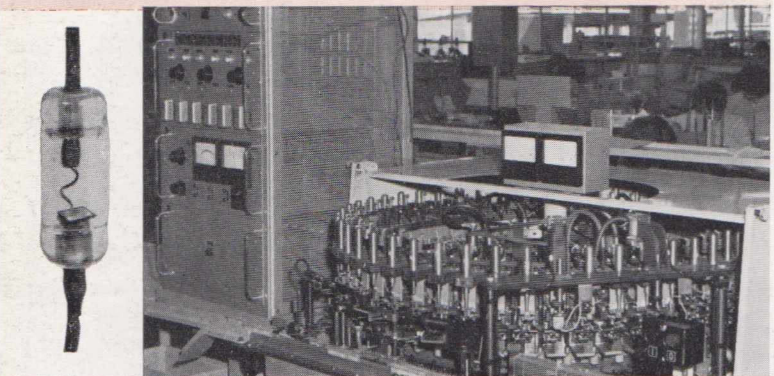

Fig. 4. A 48-head testing and sealing machine which assembles the half-diode and anode assemblies. On left is a finally sealed diode.

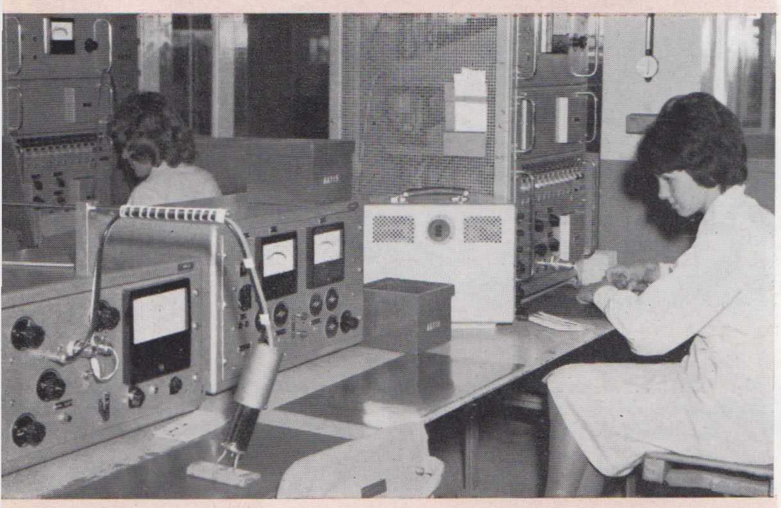

Fig. 5. Semi-automatic final test on diodes.

Quality Control

In addition to the production testing, samples are taken at various stages throughout production to control the sealing quality and the means of the electrical parameters (Figs. 6, 7 and 8).

Stringent mechanical, climatic and electrical tests are also carried out to ensure that the outgoing products have the best possible quality.

TESTING AND QUALITY CONTROL

Incoming Material Control

Testing of miniature diodes starts, naturally, with tests done on the original materials. This is normally called incoming material control.

All glass components are checked for thermal expansion and homogeneity while wire is checked for purity, uniformity and surface finishing. Crystals are checked for resistivity and orientation. Auxiliary materials, such as chemicals, are tested according to the importance they will play in the process.

Process Control in the Factory

During production of the diode, checks are made at various stages to ensure that the rejection rate will be kept to a minimum and that the manufacturing quality will be as uniform as possible.

The anode assembly is checked for welding quality, shape and whisker cross-sectional shape on point of whisker, and alignment of whisker point with anode shank. This last point is very important since the assembly is done on an automatic machine.

The cathode assembly has various samples sectioned to keep control on the thickness of the solder used to fix the germanium wafer on to the cathode holder (see front cover). This is most important in the determination of Kappa and hence the thermal stability of the diode at elevated temperatures. The sealing quality is also tested by polarised light to ensure that glass cracks will not occur later in the life of the diode, thus leading to premature failure.

After assembly in the 48-head sealing machine, the assembled diode has a second seal on the anode wire checked visually, and general alignment is also checked at this time.

After the diode has been lacquered and the leads tinned it is subjected to a 100% visual inspection and a statistical paint adhesion test.

All the tests done on process control are carefully analysed and relevant ones are charted on process control graphs with action limits being applied where necessary.

Electrical Testing

The diode, after lacquering and tinning as mentioned above, is subjected to a 100% factory test on selected parameters. These parameters include reverse leakage current at various reverse voltages up to the peak rating, and forward voltage drop at various values of forward current up to a maximum forward current rating. In addition, the breakdown voltage is tested and, depending on the type of diode being made, any other relevant parameters are measured. For example, all OA90 diodes are tested at 30 Mc/s in a typical video detector circuit in accordance with the published data sheets. As another example, the OA95 is tested for leakage currents at elevated ambient temperatures since this type has specifically a low reverse leakage current.

The diode, after branding and a further general inspection, is stored until required for delivery. Upon delivery each box has a statistical test applied to it. Various AQL's are used depending on whether the diode shows as non-operative or merely deviating from the normal requirements. Batches failing on any test are fully tested 100% and all results are carefully recorded. All records are analysed by the Quality Laboratory and a very careful check is kept on the overall outgoing quality.

Quality Control

In addition to the normal tests performed in the factory, the Quality Control Laboratory removes samples at regular intervals from the production line. These are tested for many parameters additional to those being checked in the factory. All diodes, for instance, are tested at elevated temperatures for leakage current and performance generally in the conditions which they will be expected to receive in the field. Also extensive life testing (Fig. 8) is done at elevated temperatures and maximum ratings.
In addition to all the electrical testing, the mechanical and climatical performance of the diode is checked. The diodes are subjected, amongst others, to the following types of test:—

Bending and pulling test
Vibrations test
Temperature cycling tests
High temperature storage tests
Shock loading tests
Humidity tests
Lead solderability tests
Paint and brand adhesion tests.

In general, the American and British military standards are followed very closely and a standard is aimed at which is at least as good as that required by the above-mentioned specifications.

The results of all these tests are correlated every three months into a total spread graph for each parameter over that period. These results are then combined with those of other manufacturing centres so that comparisons can be made of the relative qualities between centres making the same type. This serves as a very useful guide as to the ultimate qualities that may be aimed at for a particular product, and by inter-centre co-operation the overall benefit to all centres is quite considerable.

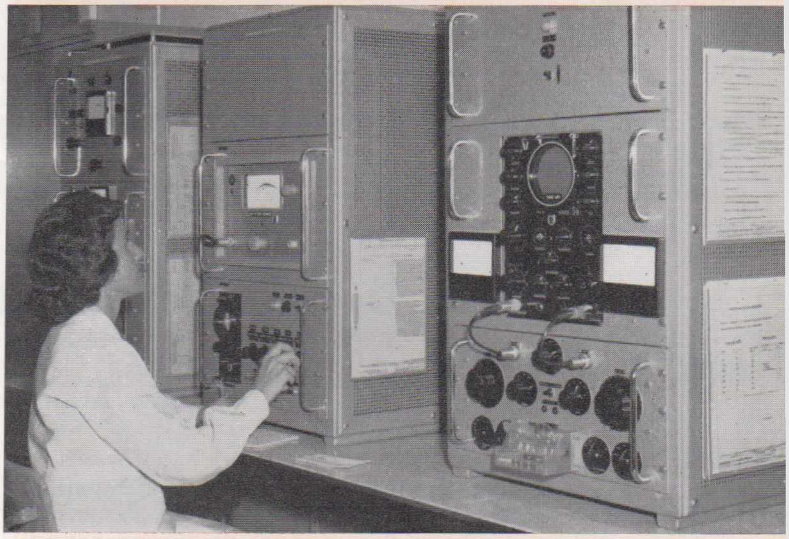

Fig. 6. Laboratory sample testing—a dynamic check being made on pairing of 2-AA119 under operating conditions.

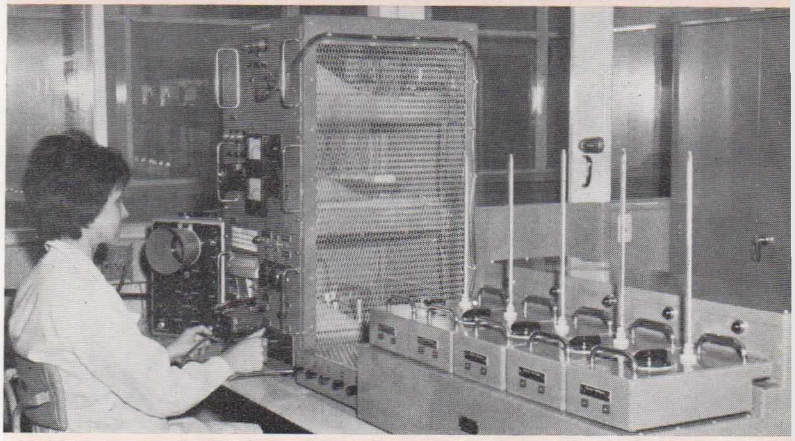

Fig. 7. Laboratory measurement of thermal resistance, an important factor in determining reliability.

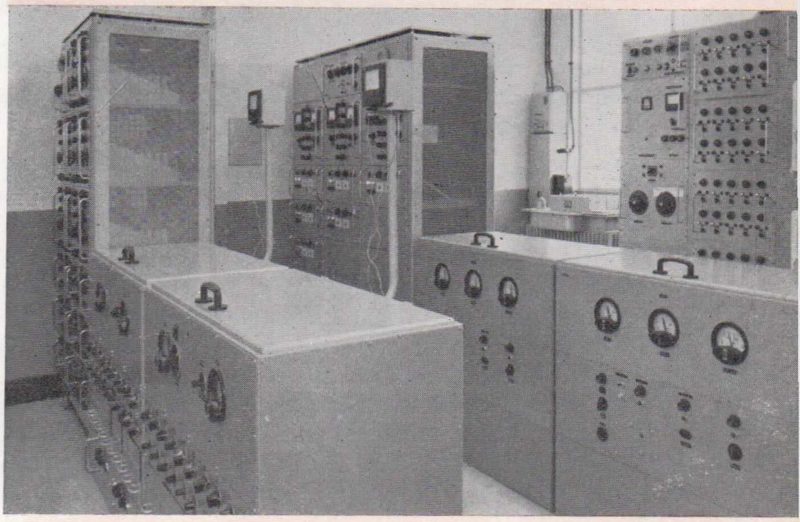

Fig. 8. Part of life test installation—the heart of any reliability programme introduced to approve release of new types.

Class B Complementary-Symmetry Amplifiers

Introducing the New Miniwatt Transistors AC 127 and AC 132

The application of the Miniwatt complementary pair of transistors AC127/132 to audio output stages eliminates the need for driver and output transformers. In applications where it is desired, a considerably improved frequency response can also be obtained. Two amplifiers are described for 9 and 12 V operation, capable of 300 mW and 500 mW output power respectively, with 5% total distortion.

The basic principles of complementary-symmetry have been adequately dealt with in the literature, e.g.,[1]. Whilst the use of a complementary-symmetry output stage offers the advantages of:

(a) economies due to savings in cost of driver and output transformers;

(b) weight and space saving, particularly important in portable apparatus;

(c) improved frequency response,

this system has not, in the past, received the local popular acceptance of conventional Class B output stages. Essentially, this has been due to the lack of suitable matched PNP and NPN transistors capable of delivering output powers of the order of 500 mW.

The recently introduced Miniwatt complementary transistor pair AC127/132 now presents very real opportunities in this field since it is theoretically possible to achieve an output power of 900 mW at a maximum ambient temperature of 45°C. In practice, however, design problems are posed due to restrictions in regard to currently available battery voltages, and speaker impedances[2].

Battery and speaker manufacturers are now showing interest and it is anticipated that a considerably wider range will soon become available. It is not the purpose here to enter into a full discussion of the economics which affect battery voltage choice, but one guiding principle is that for batteries of equal energy capacity, the end-user cost in pence per watt-hour will not vary significantly for various battery voltages. Assuming a specified power output, a design based on a higher battery voltage will result in an improved input current sensitivity at the base of the driver transistor.

Since several important design considerations are not adequately covered in the available literature, these will be briefly discussed.

Medium Power AF Output Stages Using the AC 127/132 with Battery Voltages of 9 and 12V

The description follows of two complementary-symmetry Class B output stages. The 9 and 12 V versions shown in the circuit diagram (Fig. 1) are capable of 300 and 500 mW output respectively with a total distortion of 5%.

On comparing the circuits of Fig. 1 with the basic complementary-symmetry configuration of Fig. 2a, it is seen that the AC feedback permitted by R_A has been eliminated by suitable decoupling (R_8, R_{14}, C_7). Thermal stabilisation of the output transistor emitter currents (I_{E3} and I_{E4}) has been improved by use of an NTC resistor (R_{11}). The resistor R_{12} has been made variable to allow setting up of the potential V_A to the values indicated in the circuit. Series voltage feedback is provided between the output stage and the preamplifier via C_9, R_7 and C_5. The capacitor C_5 serves to correct phase shift at high frequencies and ensures a satisfactory margin of stability.

It is important that the impedance of the capacitor C_8, used to couple the load to the output stage is small compared with R_L, otherwise a reduction in output power will occur. A miniature etched foil capacitor is not adequately specified by capacitance and voltage rating alone, since the resistance of the electrolyte may be appreciable. Miniwatt electrolytic capacitors are completely specified[3] in this respect and a suitable component can always be selected. Capacitor data is available on request.

The circuits are designed for operation up to a T_{amb} maximum of 45°C. Higher ambient operation would require, apart from additional attention to collector dissipation, another temperature sensitive element in association with R_{12} in order to stabilise the potential V_A. Otherwise unsymmetrical clipping will restrict the maximum usable output power.

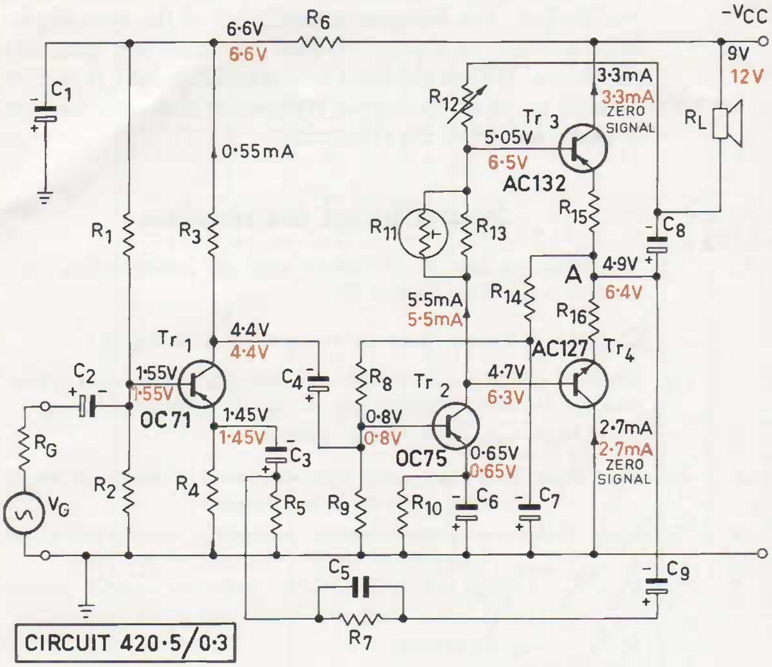

All voltages measured to ground with zero signal using a 40,000 Ω/V meter.

Components, voltages and currents of 9 V amplifier shown in BLACK

Components, voltages and currents of 12 V amplifier shown in BROWN

	9 V	12 V		9 V	12 V
R_1	39 KΩ	39 KΩ	R_{10}	120 Ω, 5%	120 Ω, 5%
R_2	12 KΩ	12 KΩ	R_{11}	NTC Philips type B8 320 01/130	B8 320 01/130
R_3	3.9 KΩ	3.9 KΩ			
R_4	2.7 KΩ	2.7 KΩ	R_{12}	1 KΩ pot.	2 KΩ pot.
R_5	10 Ω	10 Ω	R_{13}	68 Ω	68 Ω
R_6	3.3 KΩ	8.2 KΩ	R_{14}	1.8 KΩ	1.8 KΩ
R_7	2.7 KΩ	4.7 KΩ	R_{15}	3.9 Ω	2.2 Ω
R_8	4.7 KΩ, 5%	8.2 KΩ, 5%	R_{16}	3.9 Ω	2.2 Ω
R_9	1.5 KΩ, 5%	1.5 KΩ, 5%	R_L	15 Ω	25 Ω

Resistors used Philips Series B8 305 05—values required 10%, ½ W unless otherwise stated.

	9 V	12 V	Type
C_1	100 μF, 16 VW	100 μF, 16 VW	electrolytic (C426AM/E100)
C_2	10 μF, 16 VW	10 μF, 16 VW	electrolytic (C426AM/E10)
C_3	100 μF, 4 VW	100 μF, 4 VW	electrolytic (C425AL/B100)
C_4	10 μF, 16 VW	10 μF, 16 VW	electrolytic (C426AM/E10)
C_5	270 pF	390 pF	ceramic (C322BC/P270E) (C322BC/P390E)
C_6	100 μF, 4 VW	100 μF, 4 VW	electrolytic (C425AL/B100)
C_7	160 μF, 10 VW	160 μF, 10 VW	electrolytic (C426AM/D160)
C_8	250 μF, 16 VW	250 μF, 16 VW	electrolytic (C435AL/E250)
C_9	10 μF, 16 VW	10 μF, 16 VW	electrolytic (C426AM/E10)

Fig. 1. Circuit details of Complementary-Symmetry Class B amplifiers using the AC127/132.

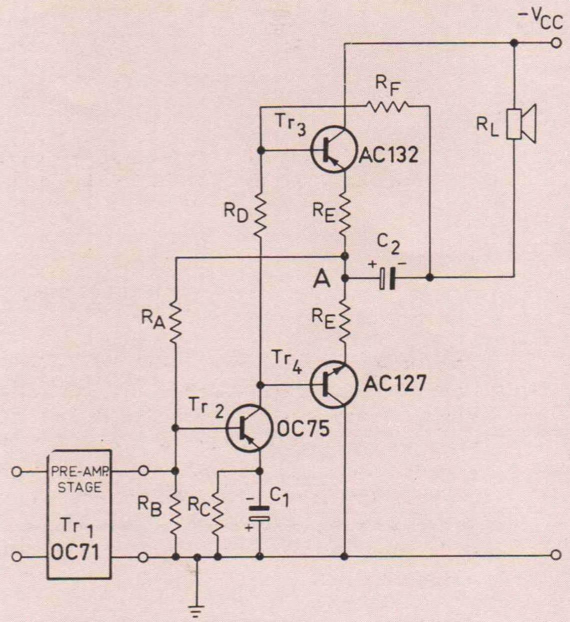

Fig. 2 (a). Basic complementary-symmetry amplifier.

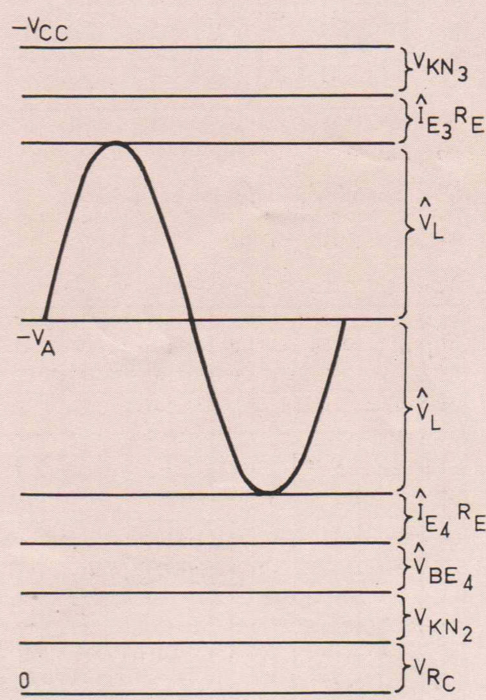

Fig. 2 (b). Dynamic operation about operating point A.

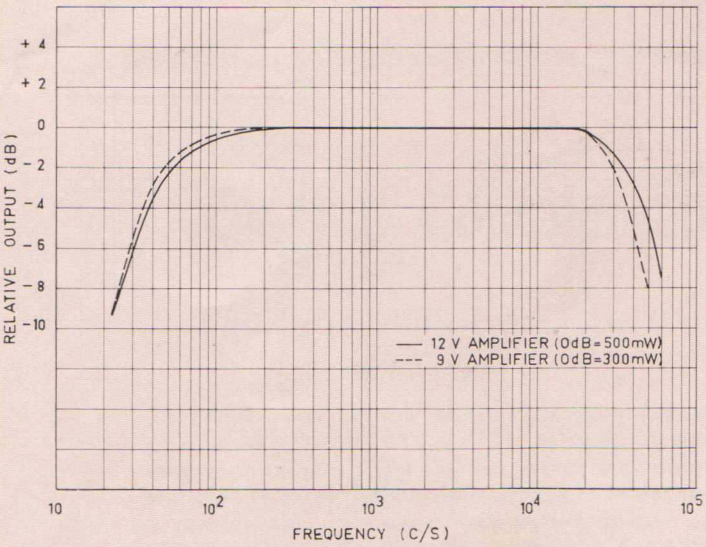

Fig. 3. Frequency response at maximum power output.

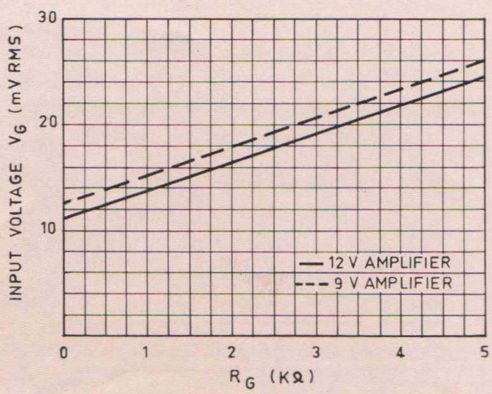

Fig. 4. Sensitivity for maximum power output.

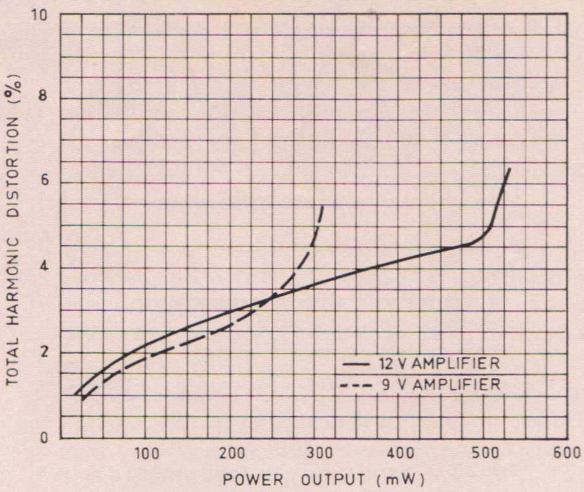

Fig. 5. Distortion characteristics at 1 Kc/s.

Graphs of frequency response, input sensitivity and harmonic distortion are shown (Figs. 3, 4 and 5 respectively). The frequency responses of the two amplifiers are far in excess of that required for portable receivers. Where the bass response is limited, it is preferable to limit the upper frequency response to give a more balanced reproduction.

General Design Considerations

The following analysis should be carefully considered in conjunction with Figs. 2a and 2b.

Glossary of Terms (used in conjunction with Fig. 2)

Numeral subscripts associated with voltages and currents correspond to transistor designations in circuit diagrams.

V_{KN2}, V_{KN3}, V_{KN4} .... *"knee" voltages.*

$\hat{V}_{BE2}$, $\hat{V}_{BE3}$, $\hat{V}_{BE4}$ .... *peak base-to-emitter voltages at maximum output power.*

V_{BE3}, V_{BE4} .... *base-to-emitter potentials corresponding to quiescent emitter currents I_{E3} and I_{E4}.*

V_{RC} .... *voltage across R_C due to quiescent emitter current I_{E2}.*

V_{CC} .... *supply voltage.*

$\hat{V}_L$ .... *peak voltage across load R_L at onset of clipping.*

V_{LOSS} .... *total voltage signal losses in output circuit which reduce available power delivered to the load.*

$\hat{I}_{E3}$, $\hat{I}_{E4}$ .... *peak emitter currents.*

I_{C2} .... *quiescent collector current.*

I_{E2}, I_{E3}, I_{E4} .... *quiescent emitter currents.*

$\hat{I}_{B3}$ .... *peak base current.*

$\hat{I}_{C3}$, $\hat{I}_{C4}$ .... *peak collector currents.*

Maximum usable power is obtained at the onset of clipping due to bottoming of transistors Tr_3 and Tr_2 and not with Tr_4 (as might have been expected) since

$V_{KN4} < V_{RC} + V_{KN2} + \hat{V}_{BE4}$.

In consequence, the quiescent potential at point A with respect to earth, i.e., $-V_A$, (Figs. 1 and 2) is not $-\frac{V_{CC}}{2}$, but is determined on the basis of symmetrical clipping of the output voltage waveform.

It can be shown that

$$V_A = \frac{V_{CC} - V_{KN3} + \hat{V}_{BE4} + V_{KN2} + V_{RC}}{2} \quad \ldots \quad (1)$$

The maximum output power into the load R_L is given by

$$P_O = \frac{\hat{V}_L^2}{2R_L} \quad \ldots \quad (2)$$

also

$$\hat{V}_L = \frac{V_{CC} - V_{LOSS}}{2} \quad \ldots \quad (3)$$

where V_{LOSS} is defined as the total voltage signal losses in the output circuit due to knee voltages, V_{BE4} and V_{RC}, and voltage drops across unbypassed emitter resistors, which reduce the available power into the load.

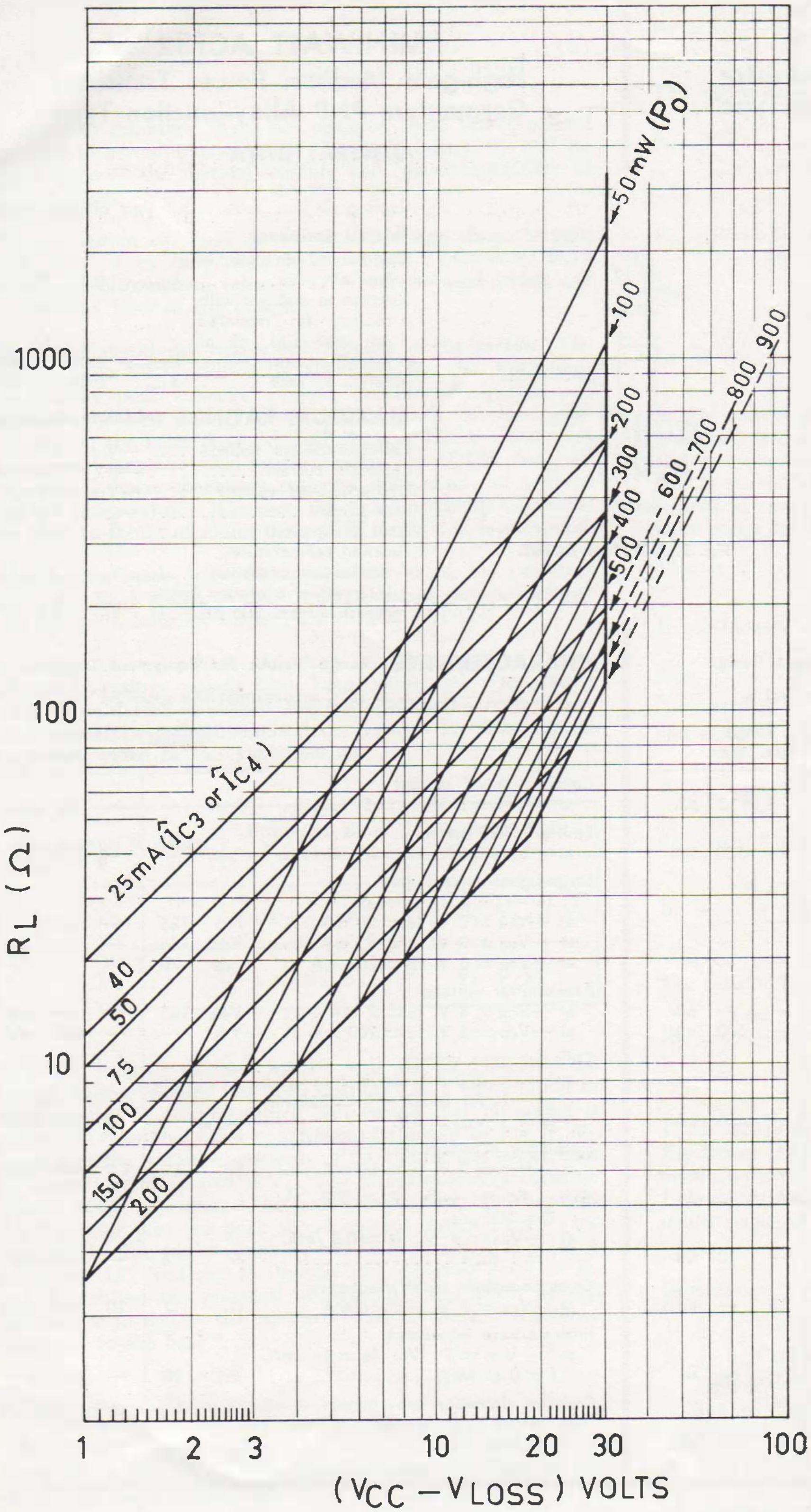

Fig. 6. Initial Design Nomograph.

Rapid Design Chart for AC127/132

technical data (abbreviated tentative data)

MINIWATT AC127

High-gain Medium Power Transistor
Germanium NPN Alloy-junction Type

GENERAL DATA

Outline (see Fig. 1) TO1
Cooling fin .... Part number 56200

Thermal Resistance

Junction to ambient in free air	K_{j-amb}	0.37	°C/mW
Junction to ambient with cooling fin mounted on heat sink of at least 2 sq. ins.	K_{j-amb}	0.16	°C/mW
Junction to case	K_{j-c}	0.11	°C/mW

MAXIMUM RATINGS (Absolute Maximum)

Collector-to-base voltage	V_{CB}	32	V
Collector current	I_C	300	mA
Emitter-to-base voltage	V_{EB}	10	V
Base current	I_B	10	mA
Total dissipation	P_{tot}	280	mW
Junction temperature:			
continuous operation	T_j	75	°C
intermittent operation (total duration max. 200 hrs.)	T_j	90	°C

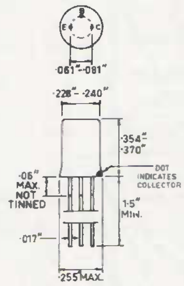

Fig. 1. AC127 or AC132.

MINIWATT AC132

High-gain Medium Power Transistor
Germanium PNP Alloy-junction Type

GENERAL DATA

Outline (see Fig. 1) TO1
Cooling fin .... Part number 56200

Thermal Resistance

Junction to ambient in free air	K_{j-amb}	0.3	°C/mW
Junction to ambient with cooling fin mounted on heat sink of at least 2 sq. ins.	K_{j-amb}	0.09	°C/mW
Junction to case	K_{j-c}	0.05	°C/mW

MAXIMUM RATINGS (Absolute Maximum)

Collector-to-base voltage ...	$-V_{CB}$	32	V
Collector current	$-I_C$	200	mA
Emitter-to-base voltage	$-V_{EB}$	10	V
Base current	$-I_B$	10	mA
Total dissipation	P_{tot}	500	mW
Junction temperature:			
continuous operation	T_j	75	°C
Intermittent operation (total duration max. 200 hrs.) ..	T_j	90	°C

CHARACTERISTICS, Range Values for Equipment Design (AC127)

—at $T_{amb} = 25$°C unless otherwise specified

		Typical	Range Min.	Range Max.	
Collector cutoff current at $V_{CB} = 5$ V, $I_E = 0$	I_{CBO}	—	—	10	μA
Emitter-cutoff current at $V_{EB} = 5$ V, $T_j = 75$ °C	I_{EBO}	—	—	550	μA
Large-signal current gain $(I_C - I_{CBO})/(I_B + I_{CBO})$					
at $V_{CB} = 0$ V, $-I_E = 20$ mA ...	h_{FE}	120	—	—	
at $V_{CB} = 0$ V, $-I_E = 50$ mA ...	h_{FE}	115	—	—	
at $V_{CB} = 0$ V, $-I_E = 200$ mA ..	h_{FE}	90	—	—	
Base-emitter voltage					
at $V_{CB} = 5$ V, $-I_E = 2$ mA	V_{BE}	120	—	—	mV
at $V_{CB} = 0$ V, $-I_E = 200$ mA ..	V_{BE}	—	—	600	mV
Collector knee voltage at $I_C = 200$ mA and at that value of I_B for which $I_C = 220$ mA with $V_{CE} = 1$ V.	V_{CEK}	—	—	450	mV
Frequency at which $\lvert h_{fe} \rvert = 1$ at $V_{CB} = 2$ V, $-I_E = 10$ mA ...	f_1	2.5	1.5	—	Mc/s
Noise figure with $R_s = 500$ Ω, B = 200 c/s at $V_{CB} = 5$ V, $-I_E = 0.5$ mA, f = 1 Kc/s	F	4	—	10	dB
Common-emitter cutoff frequency at $V_{CB} = 2$ V, $-I_E = 10$ mA ...	f_{hfe}	20	10	—	Kc/s
Intrinsic base impedance at $V_{CB} = 5$ V, $-I_E = 1$ mA, f = 0.45 Mc/s	$\lvert z_{rb} \rvert$	70	—	—	Ω
Collector depletion capacitance at $V_{CB} = 5$ V, $-I_E = 0$ mA, f = 0.45 Mc/s	c_c	70	—	—	pF

CHARACTERISTICS, Range Values for Equipment Design (AC132)

—at $T_{amb} = 25$°C unless otherwise specified

		Typical	Range Min.	Range Max.	
Collector cutoff current at $-V_{CB} = 5$ V, $I_E = 0$	$-I_{CBO}$	—	—	10	μA
Emitter-cutoff current at $-V_{EB} = 5$ V, $T_j = 75$ °C	$-I_{EBO}$	—	—	550	μA
Large-signal current gain $(I_C - I_{CBO})/(I_B + I_{CBO})$					
at $-V_{CB} = 0$ V, $I_E = 20$ mA ...	h_{FE}	135	—	—	
at $-V_{CB} = 0$ V, $I_E = 50$ mA ...	h_{FE}	115	—	—	
at $-V_{CB} = 0$ V, $I_E = 200$ mA ..	h_{FE}	70	—	—	
Base-emitter voltage					
at $-V_{CB} = 5$ V, $I_E = 2$ mA	$-V_{BE}$	105	—	—	mV
at $-V_{CB} = 0$ V, $I_E = 200$ mA ..	$-V_{BE}$	—	—	600	mV
Collector knee voltage at $-I_C = 200$ mA and at that value of $-I_B$ for which $-I_C = 220$ mA with $-V_{CE} = 1$ V.	$-V_{CEK}$	—	—	350	mV
Frequency at which $\lvert h_{fe} \rvert = 1$ at $-V_{CB} = 2$ V, $I_E = 10$ mA ...	f_1	2.0	1.3	—	Mc/s
Noise figure with $R_s = 500$ Ω, B = 200 c/s at $-V_{CB} = 5$ V, $I_E = 0.5$ mA, f = 1 Kc/s	F	4	—	10	dB
Common-emitter cutoff frequency at $-V_{CB} = 2$ V, $I_E = 10$ mA ...	f_{hfe}	17	10	—	Kc/s
Intrinsic base impedance at $-V_{CB} = 5$ V, $I_E = 1$ mA, f = 0.45 Mc/s	$\lvert z_{rb} \rvert$	90	—	—	Ω
Collector depletion capacitance at $-V_{CB} = 5$ V, $I_E = 0$ mA, f = 0.45 Mc/s	c_c	40	—	—	pF

MATCHED COMPLEMENTARY PAIRS AC127/132

The ratio of the large-signal current gains (h_{FE}) of the two transistors, at $V_{CB} = 0$ V, $\lvert I_E \rvert = 50$ mA and $T_{amb} = 25$ °C is typical 1.1 and maximum 1.25.

Here

$$V_{LOSS} = V_{KN3} + \hat{I}_{E3} R_E + \hat{I}_{E4} R_E + \hat{V}_{BE4} + V_{KN2} + I_{E2} R_C \quad .. (4)$$

and from Eqns. 2 and 3,

$$P_O = \frac{(V_{CC} - V_{LOSS})^2}{8R_L} \quad .. (5)$$

In order to minimise V_{LOSS} the designer must direct careful attention to a compromise in the choice of resistors R_C and R_E which improve the thermal stability and interchangeability of the transistors.

The calculation of V_{LOSS} in the initial design stage is seen from Eqn. 4 to be rather indeterminate. However, from experience, an assumed value of 2.5 V can be used which can be modified later in the design.

Fig. 6 will readily provide a first estimate of the design. The working area of operation is restricted by the limitations imposed by peak collector current, collector dissipation and collector-to-emitter voltage ratings. The graph has been constructed on the basis of the AC127 data, as this transistor has a somewhat larger thermal resistance than the AC132, and consequently a lower maximum collector dissipation for a given ambient temperature. However, the graph automatically satisfies that no rating of either the AC127 or AC132 is exceeded.

Once having made some assumption for V_{LOSS}, the combinations (R_L, V_{CC}) which produce a given output power, together with the peak collector current, are seen at a glance.

In setting an upper limit of voltage working for Fig. 6 two collector-to-emitter ratings have been considered. One rating is for forward bias conditions and the other under reverse bias conditions. The ratings required of Tr_3 and Tr_4 must exceed the values given in the Table below.

Transistor Number	Forward Bias Conditions	Reverse Bias Conditions
Tr_3	$V_{CC} - V_A$	$V_{CC} - V_A + \hat{V}_L$
Tr_4	V_A	$V_A + \hat{V}_L$

Since in practice reactive loads[4] will be encountered, the highest battery voltage has been restricted to a value equal to the transistor V_{CC} rating which will ensure that no rating is exceeded under the worst conditions. Referring to Fig. 2, R_D determines the quiescent currents of the output transistors, and R_F determines the potential V_A. The driver quiescent collector current (I_{C2}) must exceed the peak base current of either output transistor plus the peak signal current drawn by R_F (see Appendix). The bias resistor R_A has been returned to point A to provide DC feedback to stabilise the operating point of Tr_2 and to stabilise the potential at point A. The effect of this feedback is to reduce the effective value of the DC resistance presented to the base[5].

R_A appears at the base as $\dfrac{R_A}{1 - A_V}$

where A_V is the DC voltage gain between the base of the driver and point A (Fig. 2).

It can be shown that $A_V \approx -\dfrac{R_F + \frac{R_E}{2}}{2}$

Appendix (Refer Fig. 2)

The Eqn. 2 for output power can be expressed alternatively as

$$P_O = \frac{(V_{CC} - V_A - V_{KN3} - \hat{I}_{E3} R_E)^2}{2R_L} \quad .. \quad .. (6)$$

The maximum collector dissipation of Tr_3 and Tr_4 is given by

$$P_{C3} = \frac{(V_{CC} - V_A)^2}{\pi^2 (R_L + R_E)} + \frac{(\pi - 2)}{2\pi} I_{E3} (V_{CC} - V_A) \quad .. (7)$$

and

$$P_{C4} = \frac{V_A^2}{\pi^2 (R_L + R_E)} + \frac{(\pi - 2)}{2\pi} I_{E4} V_A \quad .. (8)$$

Also,

$$I_{C2} \geqq \hat{I}_{B3} + \frac{\hat{V}_{BE3} + \hat{I}_{E3} R_E}{R_F} \quad .. \quad .. \quad .. (9)$$

As the current gain of the driver transistor decreases rapidly at very low currents, which causes second harmonic distortion, and in order to take account of shift of driver operating point due to spread of transistor characteristics, the driver collector current should be taken about 0.4 mA higher than the lower limit given by Eqn. 9.

That is,

$$I_{C2} = 0.4\text{mA} + \hat{I}_{B3} + \frac{\hat{V}_{BE3} + \hat{I}_{E3} R_E}{R_F} \quad .. \quad .. (10)$$

Also

$$V_{RF} \approx V_{CC} - V_A - I_{E3} R_E - V_{BE3} \quad .. \quad .. (11)$$

and since

$$R_F \approx \frac{V_{RF}}{I_{C2}}$$

then from Eqns. 10 and 11,

$$R_F = \frac{V_{CC} - V_A - I_{E3} R_E - V_{BE3} - \hat{I}_{C3} R_E - \hat{V}_{BE3}}{\hat{I}_{B3} + 0.4 \times 10^{-3}}$$

The resistor R_D can be calculated from

$$R_D = \frac{V_{BE3} + V_{BE4} + R_E (I_{E3} + I_{E4})}{I_{C2}}$$

(This article is based on work carried out in the "Miniwatt" Electronic Applications Laboratory by T. Davis and in the Semiconductors Electrical Development and Application Laboratory Nijmegen by A. M. Peters and A. M. Aelbers who, whilst engaged in parallel work, reached similar conclusions.)

References

1. R. F. Shea, Transistor Circuit Engineering (Pt. 4).
2. J. R. Goldthorp, *Proc. I.R.E. Aust.*, March 1958, p. 127, correspondence.
3. Philips Electrolytic Capacitors, *Miniwatt Digest*, Vol. 1, No. 7, April 1962.
4. C. F. Wheatley & J. W. Englund, Reliability Considerations in the Applications of Power Transistors to Consumer Products, *I.R.E. Trans. on Broadcast and TV Receivers*, July 1962, p. 65.
5. M. Joyce & K. Clark, Transistor Circuit Analysis, Ch. 3.
6. C. F. Wheatley, *Electronic Design*, August 6 and September 17, 1958.

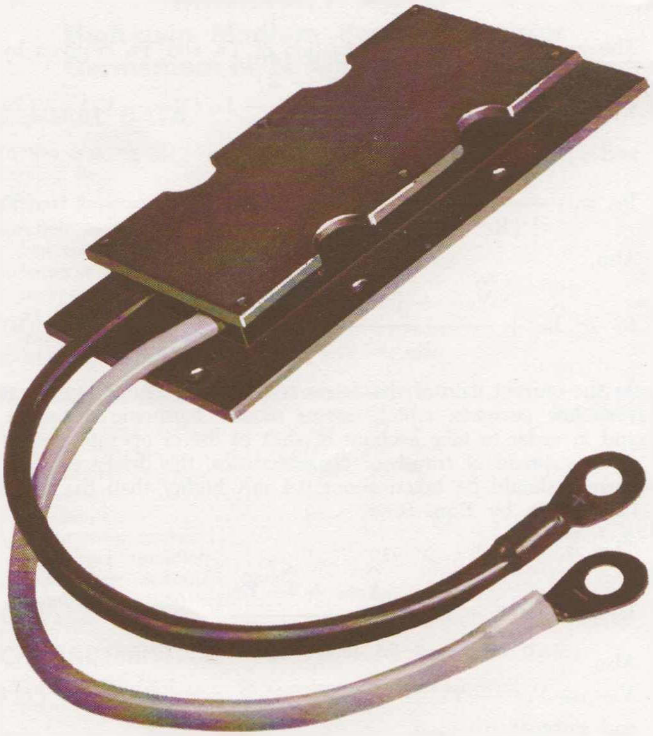

Fig. 1. Philips Peltier Battery Type PT 20/20.

Introducing

Philips Peltier Devices for Thermoelectric Cooling

Semiconductor cooling elements—and batteries of elements—using the Peltier effect are described. A battery which has a cooling power of approximately 13 W for a temperature difference between hot and cold plates of 20°C is treated in greater detail.

References are given which describe earlier work in the thermoelectric field, and which contain all basic concepts and definitions required. Typical uses of thermoelectric cooling elements are listed.

RECENT ADVANCES IN PELTIER COOLING

During recent years, a renewed interest in thermoelectricity has been in evidence. Before this, engineering interests were wholly centred on the voltage developed at the junction of dissimilar metals—the *Seebeck effect*—for the measurement of temperature and RF power. The practical application of the converse effect — in which the passage of a current through such a junction cools the junction — the *Peltier effect*, was quite out of the question. However, an outcome of modern solid state electrical and thermal transport studies has been the selection of efficient semiconductor thermoelectric alloys and compounds.

The considerably higher *thermal emf coefficient* of the selected materials compared with metals, the ability to control semiconductor resistivity via the current carrier density and to lower the specific thermal conductivity without seriously affecting the mobility of the current carriers (by using suitable alloys)—have all contributed to a considerably enhanced *figure of merit* of semiconductor Peltier devices compared with the earlier metallic thermo-pairs.

Philips Peltier devices utilise semiconductor thermopairs, comprising p-and-n type modified bismuth telluride. These possess high figures of merit as cooling elements, and make refrigeration of small volumes and local (surface) cooling a practical proposition. In general, it can be said that wherever cooling is required to no more than 50 to 60°C below room temperature, and where small volume, light weight and ease in regulating are more important than the highest efficiency of cooling, Peltier cooling stands an excellent chance of meeting all specific requirements. The efficiency of compressor type units decreases with decreasing size, and in the limit such units are just not available. This limitation does not, however, apply to Peltier cooling devices, and hence their advantages in smaller-scale cooling applications. The ability to freely dispose regions of higher or lower degrees of cooling by suitable placement of the small light Peltier elements is also an advantage.

A Peltier cooling device is essentially electronic; it has no moving parts and does not involve transport of a refrigerant. Consequently, the degree of reliability and life expectation is high. Furthermore, its application is not restricted by gravity forces, and the cooling is controllable (electronically) by varying the applied current.

Amongst typical applications of Peltier cooling are listed:

- portable domestic coolers and small air conditioners.
- portable coolers for medical or biological preparations such as plasma and bacteria cultures.
- cooling of electronic components, such as transistors.
- cooling of vacuum pump baffles.
- constant temperature enclosures (e.g., 0°C reference enclosures for thermocouple cold junctions).
- automatic dew point measuring equipment.
- measurement of heat losses from surfaces such as lagged steam pipes.
- cooling of microscope slides and microtome knives.
- beverage vending machines (e.g., for coffee extract, milk or fruit juices which have to be stored at 5°C).
- chemical distilling apparatus and temperature controllers.
- specialised cooling equipment (such as for infra-red detectors to improve signal-to-noise).

Heaton[1] has traced the historical development of thermoelectrical engineering up to the present day, and both he and Lechner[2] have provided all the basic concepts and definitions required in the practical application of the Peltier cooling devices to be described. However, some care has to be exercised to ensure correct interpretation of authors symbols. In particular, attention should be paid to η which one author uses to denote the Seebeck or thermal emf coefficient, whereas the other uses it to denote the efficiency of a Seebeck thermoelectric generator. In yet other treatments, η denotes an efficiency, or coefficient of performance (c.o.p.) for a Peltier cooling device. This is the case here where η in Fig 4 refers to $\frac{Q_c}{P}$, where Q_c is the rate at which heat is absorbed at the cold junction (*cooling power* or *heat loading capacity*) and P is the electrical power supplied to the unit.

Although dealt with in the references given [1], [2], it is thought that it would be as well to define *figure of merit* in an article of this nature. It is defined as follows:

$$Z = \frac{\alpha^2}{\lambda\rho} \text{ for a single element}$$

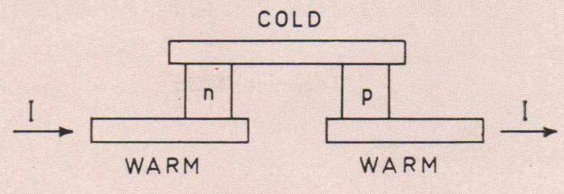

Fig. 2. Semiconductor Peltier Unit.

where
- α is the absolute thermal emf (Seebeck coefficient) V/°C
- ρ is electrical resistivity Ω/m
- λ is specific thermal conductivity W/m² per °C/m

—the units of Z thus being °C⁻¹.

or

$$Z_{np} = \frac{(\alpha_n + \alpha_p)^2}{[\sqrt{(\lambda_n\rho_n)} + \sqrt{(\lambda_p\rho_p)}]^2}$$

for a thermo-pair of p-and-n type semiconductor elements.

CONSTRUCTION OF SEMICONDUCTOR PELTIER DEVICES

The n-and-p type elements of a thermo-pair are interconnected using a bridge of high conductivity metal. Similar metallic connections are made to the remaining ends as shown in Fig. 2.

With the passage of current in the direction indicated, hot and cold junctions will be formed as illustrated. On current reversal, the cold and warm junctions will be interchanged.

By connecting together a number of units electrically in series, but thermally in parallel, a Peltier battery will be formed. This is obtained by alternating p-and-n elements and soldering copper straps between them zig-zag fashion. This results in a row of cold electrodes on one side and a row of warm ones opposite. Extremely thin layers of electrical insulation (of low thermal resistance) are then used to electrically insulate individual strapping pieces, both from each other and from the external cold and warm plates.

PHILIPS PELTIER BATTERY PT 20/20

Technical Data

Limiting Values

Current
- max. peak voltage during 5 sec .... 30 A
- max. ripple content (refer also to page 63) 10%

Insulation resistance between plate
- surfaces and connecting cables .... > 100 KΩ

Max. peak and direct voltage between
- terminals and plate surface .... 20 V

Max. temp. of hot side .... 95°C

Characteristic Data

(refer also to Fig. 4)

Optimum working current for Q_c max. .... 20 A*
Voltage at optimum working current .... approx. 2 V

*water cooling of hot side will normally be required to prevent damage.

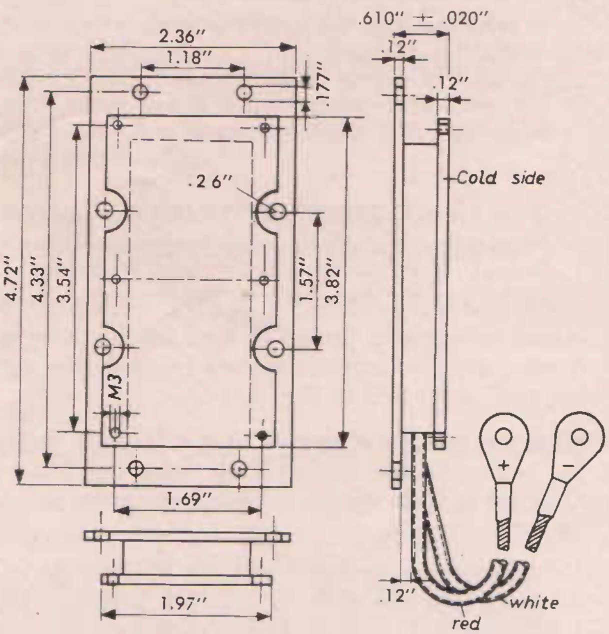

Fig. 3. Dimensional drawing of Peltier battery PT 20/20.
(The length of the terminals, including mounting tags, is 9½ ins.).

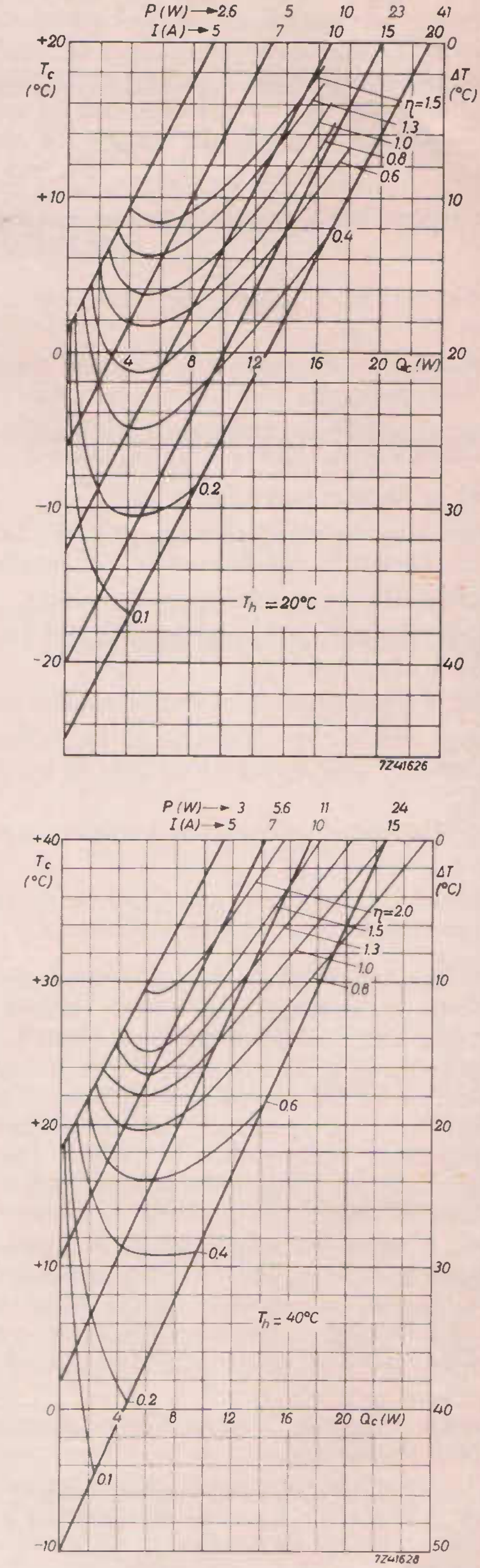

Fig. 4. Cooling capacity and current versus temperature, measured for hot-side temperatures (T_h) as indicated.

T_c = temperature of cold plate (°C)
Q_c = cooling capacity (W)
$\eta = \frac{Q_c}{P}$, P being electrical input power (W)
$\Delta T = (T_h - T_c)$

Table 1—Characteristics of the Current Range of Philips Peltier Elements

Cross-Section (mm × mm) (A)	3 ×3	3 ×3	3 ×3	3 × 5.6	3 × 5.6	5.6 × 5.6	5.6 × 5.6	5.6 × 9	5.6 × 9
Length (mm) .. .. (*l*)	4	6	8	4.2	6.8	4.2	6.8	4.2	7

Material: isotropic sintered units in p-and-n type semi-conductor.

Optimum current density: for optimum cooling capacity (i.e., for Q_c max.) ≈ 0.6 A/mm² of cross-section for 5.6 × 5.6 × 4.2 mm type (for others use $I_{opt} \propto \frac{A}{l}$). I within (10-12)% of I_{opt} is non-critical.

Resistivity: 1.3 Ω/cm.

	p-material	n-material
z value	approx. 2.6°C^{-1}	approx. 2.0°C^{-1}
α value	approx. 180μV/°C	approx. — 160μV/°C
rel. density	6.5	7.4

PHILIPS PELTIER DEVICES

Both elements and batteries are available in the Philips range.

Philips Peltier Elements

These are delivered as small blocks of rectangular cross-section with the ends specially prepared to allow soldering to the electrodes using a special low melting point (45°C) solder. The remaining surfaces are covered with a thin layer of transparent varnish. Peltier cooling is independent of the shape of element cross-section, but rectangular formation allows more efficient stacking of elements.

Their small size and weight make them particularly suitable for cooling regions which would otherwise be inaccessible. The required optimum regulating current will be the same in the case of series-connected assemblies as for individual thermo-pairs of p-and-n type material.

The reason for stacking a number of such Peltier elements for a given application, instead of using a single large element, is due to the fact that the optimum current increases with the cross-sectional area of an element.

The characteristics of the current Philips range of Peltier elements are listed in Table 1.

Philips Peltier Batteries

The current range includes three types—PT 20/20, PT 10/20 and PT 47/5.

Type PT 20/20

Philips Peltier battery PT 20/20 is a 2 V cooling unit, which comprises a series connection of 20 semiconductor thermo-elements (each 5.6 mm × 5.6 mm × 4.2 mm) consisting of n-and-p type modified bismuth telluride, mounted between two copper cover-plates.

With the passage of a DC current, one plate cools off whilst the other increases in temperature: the cold plate is differentiated in Fig. 3. The PT 20/20 has a cooling power of about 13 W for a temperature difference between the plates of 20°C.

The unit is so designed that adequate insulation is ensured. The mounting arrangements permit easy mounting of heat exchangers or water containers, and facilitate fixing to a wall of a vessel; mounting can be effected in any position. Several units can be combined in series for larger cooling capacities.

PT 20/20 units have safely withstood the following life tests:

(a) continuous operation during 2000 hours at nominal current.

(b) 3000 switchings, each of 20 mins. on and 20 mins. off, at nominal current.

(c) a commutation test: during 1000 hours the battery is operated at a temperature of 10 to 20°C on one side, and on the other side alternately 20 mins. at — 25°C and 20 mins. at + 80°C.

Notes on Use of PT 20/20

The unit should be supplied from DC, and provided with means for adequate heat removal from the hot side (a short period of operation without this will result in destruction).

If the current is derived from an AC supply, a certain amount of ripple power will be developed in the elements, half of which will appear at the cold junction, directly reducing the cooling power. Thus filtering should be adequate.

The polarity as indicated on the terminals (refer to Fig. 3) should be adhered to, and close attention should be paid to the installation instructions supplied with each battery. Reversed polarity operation is permitted provided that heat removal from the now smaller hot plate is adequate (max. temp. = 95°C) and that the current does not exceed 10 A. This permits a wide range of temperature control above, as well as below, ambient.

For soldering operations on the cold side (e.g., to improve heat transfer) low melting point (45°C) solder of special composition has to be used.

Power Supply for PT 20/20

From the data on p. 62, the recommended operation requires a low voltage, high current DC source, with ripple less than 10%. For operation from 240 V AC, a mains transformer providing 4.3 V rms a side supplying a full-wave rectifier circuit comprising two germanium diodes type OA31 will suffice.

A series choke of about 2.7 mH, designed to carry 20 A DC will provide about 2.2 V output at the stated current with 3% ripple.

Philips Peltier Batteries Available Shortly

PT 10/20

20 A* unit containing 10 thermo-pairs each of 5.6 × 5.6 × 4.2 mm.

PT 47/5

5 A* unit containing 47 thermo-pairs each of 3 × 3 × 4 mm.

* (*water cooling of hot side will normally be required to prevent damage*).

Both types have approximately the same cooling capacity, and can be provided in an alternative execution in which the cold side is fitted with a number of copper cooling extensions for direct heat exchange with liquid or gas.

References:

1. Heaton, A. G., Thermo-Electrical Engineering, *Proc. I.E.E.*, Paper No. 3867, May 1962, 109**B**, pp. 223-232.
2. Lechner, W., A Cooling Thermostat Based upon the Peltier Effect, *Philips Matronics*, July 1961, No. 19, pp. 372-377.

PHILIPS

- ELECTRONIC VALVES AND TUBES
- SEMICONDUCTOR DEVICES
- CATHODE-RAY TUBES
- LIGHT-SENSITIVE DEVICES
- TEMPERATURE-SENSITIVE DEVICES
- FERRITES
- RADIATION-SENSITIVE DEVICES
- FINE WIRES
- SPECIALIZED COMPONENTS AND DEVICES
- SPECIALIZED MATERIALS
- TECHNICAL PUBLICATIONS

For Use in the Fields of—

ENTERTAINMENT — COMMUNICATIONS — INDUSTRY
COMMERCE — MEDICINE — SCIENTIFIC RESEARCH
AND DEFENCE

PHILIPS

THE *Miniwatt* ELECTRONICS DIVISION

of

Philips Electrical Industries Pty. Limited
20 Herbert Street, Artarmon, N.S.W.
Phone 43 2171

Branches at:—

ADELAIDE	11-13 West Terrace, Adelaide, S.A., phone 51 6051
BRISBANE	56-58 Cordelia Street, South Brisbane, Qld., phone 42 471
CANBERRA	C.B.C. Chambers, Petrie Street, Civic Centre, Canberra City, A.C.T., phone J 4498
HOBART	73 Brisbane Street, Hobart, Tas., phone 3 3038
MELBOURNE	252 Sturt Street, South Melbourne, Vic., phone 69 0141
NEWCASTLE	194 Parry Street, Newcastle West, N.S.W., phone MA 5001
PERTH	672 Murray Street, Perth, W.A., phone 21 3131
SYDNEY	67 Mars Road, Lane Cove, N.S.W., phone 42 1261

Production Centre—

HENDON WORKS Tapley's Hill Road, Hendon, S.A., phone 4 5021

Hogbin, Poole (Printers) Pty. Ltd., Sydney